SEE COMMENTARY

Reversal of defective lysosomal transport in NPC disease ameliorates liver dysfunction and neurodegeneration in the *npc1*$^{-/-}$ mouse

Benny Liu[a], Stephen D. Turley[a], Dennis K. Burns[b], Anna M. Miller[c], Joyce J. Repa[a,c], and John M. Dietschy[a,1]

Departments of [a]Internal Medicine, [b]Pathology, and [c]Physiology, University of Texas Southwestern Medical Center, Dallas, TX 75390

Edited by Michael S. Brown, University of Texas Southwestern Medical Center, Dallas, TX, and approved December 4, 2008 (received for review October 28, 2008)

Niemann-Pick type C disease is largely attributable to an inactivating mutation of NPC1 protein, which normally aids movement of unesterified cholesterol (C) from the endosomal/lysosomal (E/L) compartment to the cytosolic compartment of cells throughout the body. This defect results in activation of macrophages in many tissues, progressive liver disease, and neurodegeneration. In the *npc1*$^{-/-}$ mouse, a model of this disease, the whole-animal C pool expands from 2,082 to 4,925 mg/kg body weight (bw) and the hepatic C pool increases from 132 to 1,485 mg/kg bw between birth and 49 days of age. A single dose of 2-hydroxypropyl-β-cyclodextrin (CYCLO) administered at 7 days of age immediately caused this sequestered C to flow from the lysosomes to the cytosolic pool in many organs, resulting in a marked increase in cholesteryl esters, suppression of C but not fatty acid synthesis, down-regulation of genes controlled by sterol regulatory element 2, and up-regulation of many liver X receptor target genes. There was also decreased expression of proinflammatory proteins in the liver and brain. In the liver, where the rate of C sequestration equaled 79 mg·d^{-1}·kg^{-1}, treatment with CYCLO within 24 h increased C movement out of the E/L compartment from near 0 to 233 mg·d^{-1}·kg^{-1}. By 49 days of age, this single injection of CYCLO resulted in a reduction in whole-body C burden of >900 mg/kg, marked improvement in liver function tests, much less neurodegeneration, and, ultimately, significant prolongation of life. These findings suggest that CYCLO acutely reverses the lysosomal transport defect seen in NPC disease.

cholesterol | lysosome | cyclodextrin | liver X receptor

Niemann-Pick type C (NPC) disease results from mutations that inactivate 1 of 2 proteins, either NPC1 (95% of cases) or NPC2 (1, 2). These 2 proteins normally act in concert to facilitate the movement of unesterified cholesterol (C), derived from the cellular uptake of lipoproteins, across the limiting membrane of the lysosome to the metabolically active pool of sterol in the cytosolic compartment (3, 4). As a consequence of these mutations, C progressively accumulates in the late endosomal/lysosomal (E/L) compartment of virtually every cell in the body from the time of early fetal development until death of the child or animal (5). In the *npc1*$^{-/-}$ mouse (6), a murine model of the common form of NPC disease, the animal sequesters an amount of sterol equal to 67 mg/kg body weight (bw) every day so that the whole-body sterol pool increases from ≈2,200 to 5,700 mg/kg between birth and 7 weeks of age (7). Pathologically, this C accumulation is associated with infiltration of activated macrophages into many organs and with parenchymal cell death. In both the human and the mouse, these histological changes, in turn, result in the clinical syndromes of pulmonary failure, liver dysfunction, and progressive neurological disease (3, 8). Importantly, in a particular organ, the severity of disease is proportional to the amount of C sequestered in that tissue (3, 9, 10).

The sterol that is sequestered in the late E/L compartment of cells in each organ is internalized through 2 different transport mechanisms involving the cellular uptake of lipoproteins through either receptor-mediated or bulk-phase endocytosis. Receptor-mediated uptake utilizes the low-density lipoprotein receptor (LDLR) that is able to bind lipoproteins containing either apolipoprotein (apo) E or apoB_{100}, such as remnants of chylomicrons and very low-density lipoprotein (VLDL), and LDL (11, 12). The velocity of this uptake process in a particular organ *in vivo* is determined by the concentration of lipoproteins in the plasma, the level of LDLR expression, the affinity constant for a given lipoprotein, and the reflection coefficient defining the permeability characteristics of the capillary membranes overlying the parenchymal cells of that tissue. The rate of uptake of lipoproteins by bulk-phase endocytosis is also determined by the concentration of the particles in the plasma and the reflection coefficient of the capillary membranes; however, in addition, it may be influenced by nonsolvent water effects within the endocytic vesicles (13). In the *npc1*$^{-/-}$ mouse, 88% of LDL cleared from the plasma and sequestered in different tissues is taken up by receptor-mediated endocytosis, whereas only 12% is cleared by bulk-phase endocytosis (7). However, when LDLR activity is eliminated, as in the *npc1*$^{-/-}$/*ldlr*$^{-/-}$ animal, all LDL is cleared by bulk-phase endocytosis. Because the rate constants for these two processes are very different in different organs, the profile of C sequestration in tissues varies markedly in the *npc1*$^{-/-}$/*ldlr*$^{+/+}$ and *npc1*$^{-/-}$/*ldlr*$^{-/-}$ animals (3). Importantly, these rate constants for lipoprotein uptake by either receptor-mediated or bulk-phase endocytosis are unaffected by the presence or absence of the NPC1 mutation. Whole-animal LDL clearance by receptor-mediated (≈520 mL·d^{-1}·kg^{-1}) and bulk-phase (≈62 mL·d^{-1}·kg^{-1}) endocytosis is approximately the same in *npc1*$^{+/+}$ and *npc1*$^{-/-}$ mice (7). However, there is evidence that the lipid accumulation seen in *npc1*$^{-/-}$ cells does lead to a 2-fold expansion of the bulk-phase volume found within the lysosomal compartment and to a diminished rate of movement of this bulk-phase fluid back out of the cell (14).

One way to take advantage of these observations to control the severity of disease caused by the NPC1 mutation is to reduce the amount of lipoprotein cholesterol available for uptake into cells. Thus, blocking the intestinal absorption of sterol with a drug like ezetimibe, which lowers the amount of C reaching the liver carried in chylomicron remnants, markedly reduces hepatocyte damage and improves hepatic function (9). Increasing sterol excretion out of the brain across the blood-brain barrier, which presumably leaves

NEUROSCIENCE

Author contributions: B.L., S.D.T., J.J.R., and J.M.D. designed research; B.L., S.D.T., D.K.B., and A.M.M. performed research; and B.L., S.D.T., J.J.R., and J.M.D. wrote the paper.

The authors declare no conflict of interest.

This article is a PNAS Direct Submission.

See Commentary on page 2093.

[1]To whom correspondence should be addressed at: Department of Internal Medicine, University of Texas Southwestern Medical School, 5323 Harry Hines Boulevard, Dallas, TX 75390. E-mail: john.dietschy@utsouthwestern.edu.

This article contains supporting information online at www.pnas.org/cgi/content/full/0810895106/DCSupplemental.

© 2009 by The National Academy of Sciences of the USA

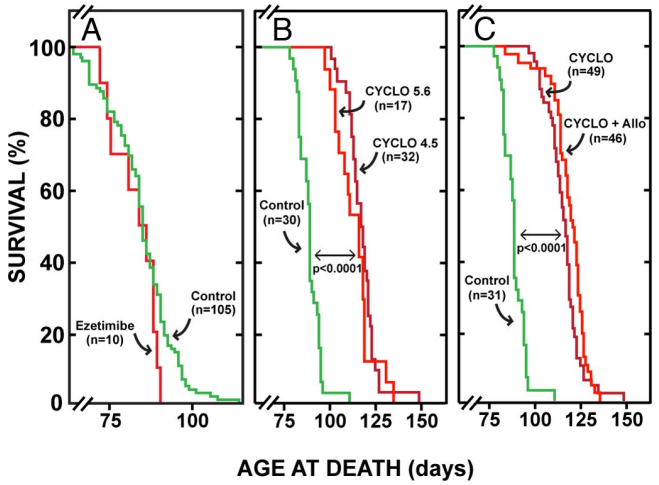

Fig. 1. Cyclo expands lifespan in the *npc1*$^{-/-}$ mouse. (*A*) *Npc1*$^{-/-}$ mice continuously fed ezetimibe, which markedly lowers cholesterol flux into the liver and improves liver function, did not live longer than those animals not fed this compound. (*B*) A single dose of CYCLO 4.5 or 5.6 administered at 7 days of age did, however, significantly and equally prolong life. (*C*) Addition of Allo to either the CYCLO 4.5 or CYCLO 5.6 did not significantly further prolong life (number indicated for each group). In each experiment, the untreated control animals were littermates of the treated group.

less apoE-associated C available for uptake by neurons, slows neurodegeneration and prolongs the life of the *npc1*$^{-/-}$ mouse (10). An alternative approach to this problem would be to deliver an agent through bulk-phase endocytosis into cells that reverses the transport defect in the late E/L compartment, and allows the sequestered C to move into the metabolically active pool, where it could be metabolized and secreted through normal mechanisms. That such a manipulation might be possible is suggested by the observation that administration of the sterol-binding agent, 2-hydroxypropyl-β-cyclodextrin (CYCLO), also slows nerve cell death and prolongs the life of the *npc1*$^{-/-}$ mouse (15, 16). Thus, the current studies were designed to investigate the molecular and biochemical effects of the acute administration of CYCLO on sterol metabolism in the neonatal mouse and, further, to examine the more prolonged alterations that this single dose of CYCLO has on the natural history of NPC disease when the animal reaches maturity. The results suggest that this compound acutely and completely overcomes the transport defect caused by the NPC1 mutation.

Results

Effect of CYCLO on Age at Death. Untreated *npc1*$^{-/-}$ mice died at an average age of 84 days (Fig. 1*A*). Treatment of these mice from birth with ezetimibe (20 mg·d^{-1}·kg^{-1}), which blocks cholesterol absorption, markedly reduced C flux into the liver and greatly improved liver function tests (9) but had no effect on longevity. However, the s.c. administration of only a single dose (4,000 mg/kg) of either CYCLO 4.5 or CYCLO 5.6 to *npc1*$^{-/-}$ pups at 7 days of age markedly prolonged lifespan (Fig. 1*B*). There was no significant difference between these 2 CYCLO preparations varying only in their degree of substitution. When allopregnanolone (Allo; 25 mg/kg), a neurosteroid, was simultaneously administered along with the CYCLO 4.5 or CYCLO 5.6, there was no significant further prolongation of life (Fig. 1*C*). Clearly, administration of the single dose of CYCLO to the 7-day-old pups had induced a major alteration in some aspect of the pathophysiology of NPC disease that had a very favorable impact on longevity.

CYCLO Pharmacokinetics. When ^{14}C-CYCLO was administered along with the dose of unlabeled compound and monitored, the molecule was cleared more slowly in the 7-day-old pups, such that after 6 and 24 h, respectively, 66% and 9% of the administered dose remained in the animals. The results were different in the 49-day-old mice, where only 8% and 3%, respectively, of the dose was found in the animals at these 2 times. From the dose of the compound administered, these data on whole-animal turnover, and rates of bulk-phase endocytosis (3), it could be calculated that the theoretical maximum amount of CYCLO taken up into the liver of the 7-day-old pups through bulk-phase endocytosis and delivered into the late E/L compartment during the 24-h interval would have equaled ≈540 mg/kg (≈14% of the administered dose). Based on these preliminary observations, all subsequent studies designed to elucidate the mechanisms involved in this marked prolongation of life were undertaken in mice given a single dose of CYCLO 4.5 (4,000 mg/kg) alone at 7 days of age.

Acute Effects of CYCLO Administration on Sterol Metabolism in Liver, Brain, and Whole Animal. Initial experiments examined the acute effects of CYCLO administered to 7-day-old animals and studied 24 h later. The 8-day-old *npc1*$^{+/+}$ pups given only saline had a slightly elevated hepatic cholesteryl ester (CE) concentration (0.86 mg/g), reflecting the increased intake of dietary C during suckling (60 mg·d^{-1}·kg^{-1}), so that the total sterol concentration (3.3 mg/g) was also marginally elevated (Fig. 2*A*). However, the 8-day-old *npc1*$^{-/-}$ pups given only saline already manifested a 5-fold increase in total hepatic sterol concentration (16.8 mg/g), nearly all of which was unesterified (16.5 mg/g). Because of the increased dietary sterol intake, hepatic synthesis in the *npc1*$^{+/+}$ pups was partially suppressed (216 nmol·h^{-1}·g^{-1}) (Fig. 2*D*). In contrast, even though the pool of C in the liver cells was markedly expanded in the *npc1*$^{-/-}$ animals, synthesis was 12-fold higher (2629 nmol·h^{-1}·g^{-1}). Although treatment of the *npc1*$^{+/+}$ pups with CYCLO had no significant effect on either of these parameters, the effects in the *npc1*$^{-/-}$ animals were very large. The markedly elevated rate of sterol synthesis was suppressed nearly to 0 (Fig. 2*D*), the concentration of C markedly decreased, the level of CE increased 14-fold (from 0.3 to 4.3 mg/g), and total sterol concentration in the liver significantly declined (Fig. 2*A*). Of note, although the synthesis of C was markedly suppressed, the synthesis of fatty acids was unchanged in CYCLO-treated (5.82 μmol·h^{-1}·g^{-1}) vs. untreated (5.83 μmol·h^{-1}·g^{-1}) *npc1*$^{-/-}$ pups. Although quantitatively less profound, similar changes were seen in the brain of the *npc1*$^{-/-}$ mice, where treatment with CYCLO increased the concentration of CE nearly 3-fold (from 0.014 to 0.041 mg/g) (Fig. 2*B*) and suppressed the rate of sterol synthesis (Fig. 2*E*). Furthermore, such changes were also seen in the remaining tissues of the carcass, which manifested increases in both the concentration of C (Fig. 2*C*) and rates of synthesis (Fig. 2*F*) in the untreated *npc1*$^{-/-}$ pups. Administration of CYCLO significantly lowered the mean concentration of sterol in these tissues and returned the rates of synthesis to those seen in the untreated *npc1*$^{+/+}$ animals.

From the weights of the individual organs and whole animals (Fig. 2*G*), these values were used to determine the effects of the NPC1 mutation and treatment with CYCLO on whole-animal sterol metabolism in these 8-day-old mice. As expected, C synthesis was significantly elevated in the untreated *npc1*$^{-/-}$ mice (299 mg·d^{-1}·kg^{-1}) compared with the untreated *npc1*$^{+/+}$ animals (157 mg·d^{-1}·kg^{-1}) (Fig. 2*I*), even though the whole-animal C pool in these pups was already greatly expanded (3,674 mg/kg) compared with the control animals (2,347 mg/kg) (Fig. 2*H*). Strikingly, only 24 h after administration of CYCLO, this expanded whole-animal C pool had been reduced by nearly 500 mg/kg and synthesis was returned to levels (138 mg·d^{-1}·kg^{-1}) seen in the *npc1*$^{+/+}$ mice. Taken together, these dramatic changes were consistent with the view that treatment with CYCLO rapidly overcame the block in sterol transport out of the late E/L compartment in the *npc1*$^{-/-}$ pups and allowed C to flow into the metabolically active pool for disposition in the cells of these organs.

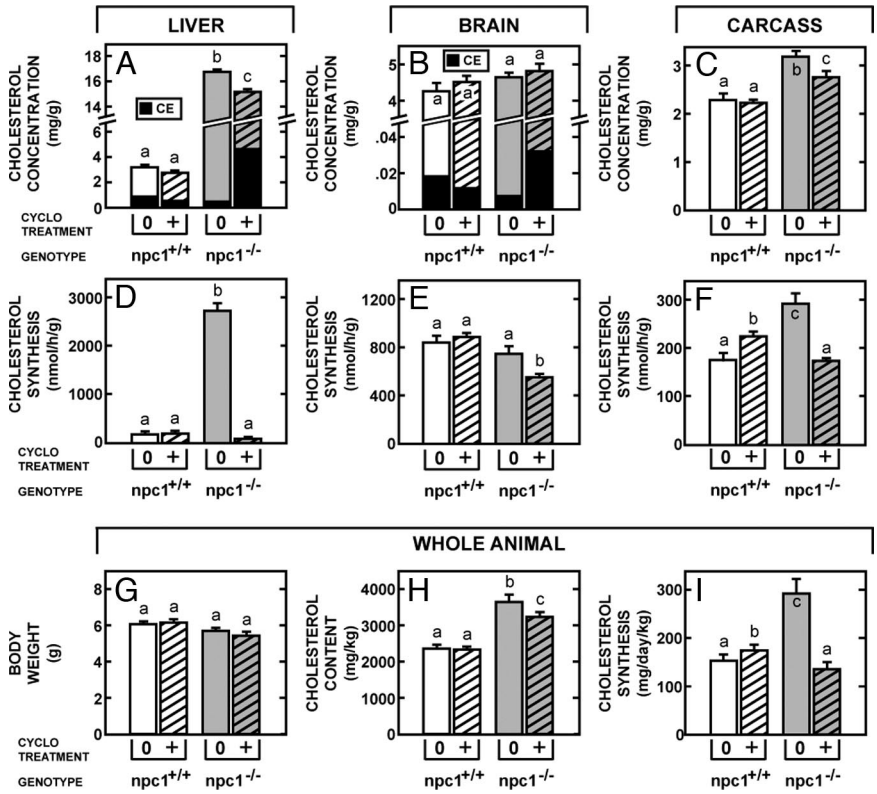

Fig. 2. A single dose of CYCLO 4.5 administered to 7-day-old pups markedly altered sterol metabolism in the *npc1*$^{-/-}$ mice 24 h later but had no effect in the *npc1*$^{+/+}$ animals. The unesterified and esterified cholesterol concentrations are shown in the liver (*A*) and brain (*B*), whereas total cholesterol concentrations are given for the remaining tissues of the carcass (*C*). (*D–F*) Cholesterol synthesis rates are shown for the same 3 tissue compartments. These values (*G*) are combined to give whole-animal cholesterol pools (*H*) and synthesis rates (*I*) in these same animals. To obtain these latter values, the rates of incorporation of ^3H_2O into sterols by the different organs were converted to absolute rates of cholesterol synthesis. Statistically significant differences are indicated by the different letters ($n = 6$, $P < 0.05$).

Acute Effects of CYCLO Administration on Major Regulatory Mechanisms in Liver and Brain. If, in fact, CYCLO treatment had promoted such a sudden efflux of C into the cytosolic compartment, there should be major changes manifested in the 2 regulatory systems in this compartment, sterol regulatory element 2 (SREBP2) and liver X receptor (LXR), known to respond to variations in the size of the metabolically active sterol pool (17, 18). Because sterol O-acyltransferase 2 in the liver is constitutive, relative mRNA levels for this gene were the same in the 4 groups of pups (Fig. 3*A*). In contrast, mRNA levels for SREBP2 and its target genes, 3-hydroxy-3-methylglutaryl coenzyme A (HMG CoA) synthase I (SYN), HMG CoA reductase (RED), and LDLR, were all significantly elevated in the untreated *npc1*$^{-/-}$ mice (Fig. 3 *B–E*). After CYCLO treatment, however, these mRNA levels were markedly suppressed, below even the levels seen in the *npc1*$^{+/+}$ pups. In contrast, mRNA expression of the LXR target genes, ATP-binding cassette (ABC) A1, ABCG1, ABCG5, ABCG8, and cytochrome P450 7A1 (CYP7A1), was not elevated in the untreated *npc1*$^{-/-}$ mice (Fig. 3 *F–J*). After CYCLO treatment, however, the expression of ABCG1 and CYP7A1 became significantly elevated. Failure to observe a change in ABCA1 mRNA levels in liver is consistent with the report that the hepatic ABCA1 transcript isoform is not under regulatory control of dietary C or LXR (19). Another characteristic feature of NPC disease of the liver is the presence of activated macrophages. This was reflected in elevated mRNA levels of a number of inflammatory factors, including CD11c, CD68, MIP-1α (chemokine ligand 3), and TLR4 but not TNF-α (Fig. 3 *K–O*). Of note, the mRNA level of TNF-α was elevated in older *npc1*$^{-/-}$ mice (20). Treatment with CYCLO also significantly reduced this overexpression. Brain showed similar changes 24 h after CYCLO administration. The relative mRNA level of SREBP2 and HMG CoA SYN was reduced (Fig. 3 *P* and *Q*), and that of the LXR target genes, ABCA1 and apoD, was significantly increased (Fig. 3 *R* and *T*). In addition, the elevated mRNA level of CD11c, reflecting activated glia in the brain, was restored to normal after CYCLO treatment (Fig. 3*S*).

Long-Term Effects in the Adult Mouse of CYCLO Administration in Infancy. The next studies were designed to identify the long-term effects, if any, in 49-day-old adult mice that had been administered CYCLO at 7 days of age. Again, CYCLO administration to the *npc1*$^{+/+}$ mice had no effect on either C concentrations or synthesis rates in the liver, brain, and other organs (Fig. 4 *A–C*). However, there were marked residual effects in the *npc1*$^{-/-}$ animals. Six weeks after administration of CYCLO, when none of the compound was retained in the body, the concentration of C was still significantly reduced in the liver, kidney, spleen, and other organs. No reduction was seen in the brain, however, because most of the C in this organ is present in myelin, so that any changes that might have occurred in neurons are obscured. In addition, in nearly every organ, including the brain, C synthesis was increased (Fig. 4 *E–G*), presumably to offset the deficit of C in the metabolic pool, because sterol was again being sequestered in the late E/L compartment. As a consequence of these changes, 6 weeks after administration of the CYCLO, the whole-animal cholesterol pool was still reduced by >900 mg/kg even though synthesis was increased by 48 mg·d^{-1}·kg^{-1} (Fig. 4 *D* and *H*).

The residual effects of this single dose of CYCLO on the clinical measures of disease were even more dramatic. The liver function tests, aspartate aminotransferase and alanine aminotransferase, were markedly improved (Fig. 4 *I* and *J*), and the level of neurodegeneration in the brain was significantly reduced. The *npc1*$^{-/-}$ mice had accumulations of vesicular storage material within the perikarya of neurons in multiple areas of the brain, most prominently in the neocortex, diencephalon, and ventral brainstem nuclei. In the cerebellum, there was marked loss of Purkinje cells, particularly in the anterior-superior cerebellar vermis, and this loss was accompanied by a proportional degree of Bergmann gliosis (Fig. 5*A* and *B*). Storage material identical to that seen in the other perikarya was present in the cytoplasm of the remaining Purkinje cells. This cell death was also strikingly expressed in loss of calbindin immunoreactivity in the molecular layer (Fig. 5 *D* and *E*), reflecting loss of Purkinje cell dendrites, and by a marked increase in GFAP

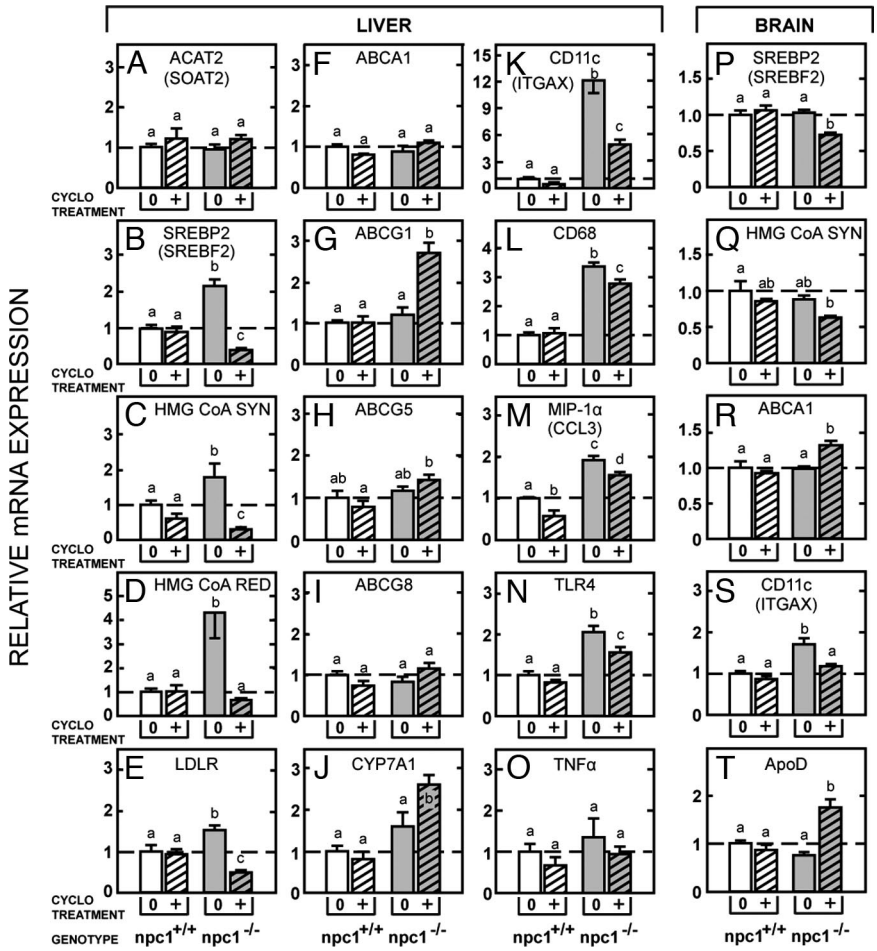

Fig. 3. A single dose of CYCLO 4.5 was administered to 7-day-old *npc1*$^{-/-}$ and *npc1*$^{+/+}$ pups, and tissues were obtained 24 h later. RNA was extracted from the liver and brain for measurement by quantitative real-time PCR. (*A*) The mRNA level for ACAT2 is shown. The mRNA levels for hepatic target genes regulated by SREBP2 (*B–E*) and LXR (*F–J*) are shown in columns 1 and 2, respectively. (*K–O*) The third column provides relative mRNA levels in liver for various inflammatory proteins. (*P–T*) The fourth column of data shows several of these same relative mRNA values in the brain. Statistically significant differences are indicated by different letters ($n = 6$, $P < 0.05$).

immunoreactivity (Fig. 5 *G* and *H*), indicating activation of glial cells in the areas of Purkinje cell loss. This neurodegeneration occurred in a band-like distribution similar to that described (21). Although the single dose of CYCLO administered at 7 days of age did not alter the number of pyramidal cells present in the cerebral cortex of these 49-day-old animals (Fig. 4*K*), the number of surviving Purkinje cells in the cerebellum was more than doubled (Fig. 4*L*, 5*C*). This beneficial effect was also reflected in the substantial increase in calbindin immunoreactivity and the reduction in GFAP immunoreactivity seen in the cerebellum (Fig. 5 *F* and *I*), compared with untreated animals.

Finally, at 49 days of age, external sterol balance in the CYCLO-treated *npc1*$^{-/-}$ mice had returned to levels seen in the untreated animals (Fig. 4 *M* and *N*). The sum of the fecal neutral and acidic sterol outputs equaled ≈190 mg·d^{-1}·kg^{-1} in both groups, which was significantly higher than the 120 mg·d^{-1}·kg^{-1} found in the untreated *npc1*$^{+/+}$ animals. Again, CYCLO administration had no effect on sterol balance in these control mice. Thus, apparently, the single dose of cyclodextrin had markedly lowered the whole-animal pool of C in the days after its administration at 7 days of age and significantly slowed the development of liver and central nervous system disease. However, by 49 days of age, this effect had worn off; the animals were again sequestering sterol at a rate of ≈70 mg·d^{-1}·kg^{-1}, and external sterol balance had returned to the elevated levels usually found in *npc1*$^{-/-}$ mice.

Discussion

To variable degrees, nearly all cells in the body take up lipoproteins carrying apoE or apoB$_{100}$. The CE present in the hydrophobic core of these particles is processed in lysosomes by a lysosomal acid lipase (LAL) to C (22), which, in turn, is moved across the limiting membrane to the metabolically active pool of sterol in the cytosolic compartment by the concerted actions of NPC1 and NPC2. Mutations that inactivate LAL lead to accumulation of CE in the lysosomal compartment (Wolman disease) (23), whereas inactivation of NPC1 or NPC2 causes the sequestration of C (NPC disease). In the *npc1*$^{-/-}$ mouse, although this mutation leads to expansion of the C pool in the late E/L compartment (4), there is a perceived shortage of sterol in the rest of the cell. As a result, there is marked activation of the SREBP2 target genes with an increase in sterol synthesis, no stimulation of the LXR target genes, and almost no CE formation (Figs. 2 and 3). In the liver, which expresses high levels of LDLR and where the reflection coefficient of the capillary bed is essentially zero, the rate of C sequestration equaled 79 mg·d^{-1}·kg^{-1} during the 8 days between birth and when these animals were studied. The rate of accumulation in the remaining tissues of the body was 87 mg·d^{-1}·kg^{-1}.

After administration of CYCLO, there were rapid changes in the distribution of sterol within cells of all tissues. In the liver, for example, the rate of C movement out of the sequestered pool of sterol suddenly increased to 233 mg·d^{-1}·kg^{-1}, a rate that was 3-fold greater than the rate of sequestration. This shift of C into the metabolically active pool was reflected in profound suppression of SREBP2 and its target genes, leading to nearly complete inhibition of *de novo* sterol synthesis, activation of the LXR target genes ABCG1 and CYP7AI, and rapid expansion of the CE pool in the cytosol (Figs. 2 and 3). Of the 233 mg of C leaving the late E/L pool during this 24-h period, most moved to the ester pool in the cytosol (174 mg·d^{-1}·kg^{-1}), whereas the remainder must have been excreted from the liver (59 mg·d^{-1}·kg^{-1}) either as C or, after conversion, to

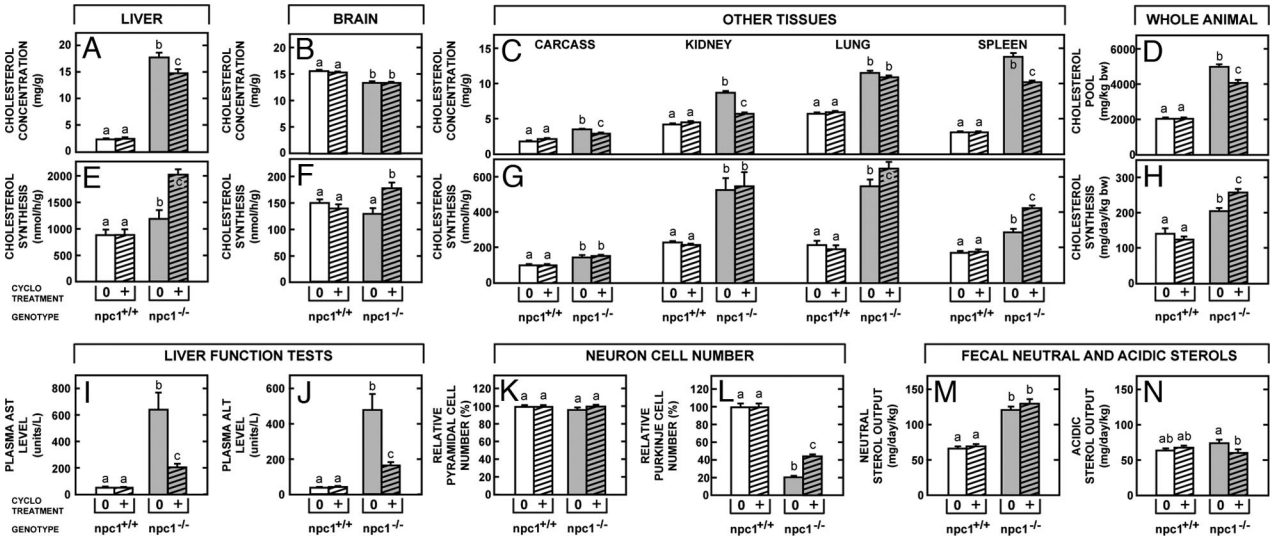

Fig. 4. *Npc1*$^{+/+}$ and *npc1*$^{-/-}$ mice were administered CYCLO 4.5 at 7 days of age and were then studied at 49 days of age. Total cholesterol concentrations were determined in liver (*A*), brain (*B*), and various other tissues (*C*), and these were combined to give whole-animal cholesterol pools (*D*). Similarly, cholesterol synthesis was measured in these same tissues (*E–G*), and these data were combined to give whole-animal synthesis rates (*H*). In these same groups of animals, liver function tests were also measured (*I* and *J*), pyramidal and Purkinje cell numbers were quantitated in the brain (*K* and *L*), and daily fecal neutral and acidic sterol output was determined (*M* and *N*). Statistically significant differences are indicated by different letters ($n = 6$, $P < 0.05$).

bile acid. In this manner, the hepatocytes attempted to adjust for the sudden influx of C into the metabolically active pool by immediately suppressing synthesis, sequestering much of the excess C as relatively inert CE, and excreting the remainder into bile. Similar, although less dramatic, changes were identified in the brain and remaining tissues of the body (Fig. 2). As a result, within only 24 h of administration, CYCLO had reduced the total C pool in the 8-day-old pups by nearly 500 mg/kg. Presumably, this increase in net excretion continued for several more days until the CYCLO was fully excreted from the body.

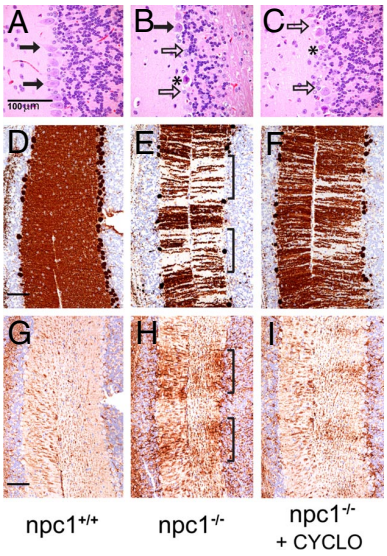

Fig. 5. Representative histological sections are shown of anterior-superior cerebellar vermis from 49-day-old *npc1*$^{+/+}$ (*A*, *D*, and *G*), *npc1*$^{-/-}$ (*B*, *E*, and *H*), and *npc1*$^{-/-}$ mice treated with CYCLO 4.5 at 7 days of age (*C*, *F*, and *I*). Contiguous sections were stained with H&E (*A–C*) or for calbindin (*D–F*) or GFAP (*G–I*) immunoreactivity. There was substantial loss of Purkinje cells (solid arrows) in untreated *npc1*$^{-/-}$ animals (*B*), which was partially prevented by treatment with CYCLO 4.5 (*C*). (*B* and *C*) Increased numbers of Bergman glia (open arrows) and necrotic Purkinje cells (*) were also visible in the untreated *npc1*$^{-/-}$ mice. (*E*) Calbindin immunoreactivity was markedly decreased in a band-like pattern in the molecular layer of untreated *npc1*$^{-/-}$ animals (brackets) reflecting loss of Purkinje cell dendrites. (*H*) In contrast, there was increased GFAP immunoreactivity in the molecular layer in the same regions of calbindin loss (brackets) reflecting activation of astrocytes. Treatment with CYCLO 4.5 markedly reduced this loss of calbindin expression (*F*) and diminished GFAP expression (*I*). (Measurement bars: 100 μm.)

CYCLO is a hydrophilic molecule containing a lipophilic pocket capable of solubilizing C and other hydrophobic molecules (24). It facilitates the movement of C between membranous structures by reducing the activation energy for desorption of the C molecule from ≈20 kcal/mol to 7 kcal/mol (25). Depending on the concentration and molar ratio of CYCLO to C, a solution of this molecule can either extract sterol from cell membranes (CYCLO/C molar ratio of >60) or enrich the membrane with C (molar ratio <60) (26). In addition, at low concentrations (<1 mM), CYCLO can act catalytically, markedly enhancing the rate of molecular exchange of C between different hydrophobic compartments (27). Thus, one way in which CYCLO might have acted in the *npc1*$^{-/-}$ mice was to extract C from the plasma membranes of cells, facilitating its elimination from the body as the CYCLO was excreted by the kidneys. This is almost certainly not the case, however, in that there is no known pathway for C to move from the late E/L compartment directly to the plasma membrane in the *npc1*$^{-/-}$ cells. In addition, such a process would invariably lead to an increase in C synthesis and a reduction in the level of CE in cells. Importantly, no such effects were seen in the *npc1*$^{+/+}$ animals receiving CYCLO (Figs. 2 and 3), and in the *npc1*$^{-/-}$ mice, synthesis was actually suppressed, whereas the pool of CE was markedly expanded. A second possibility is that the CYCLO, reaching the late E/L compartment through bulk-phase endocytosis, altered the permeability of the limiting membrane in a nonspecific fashion, allowing C and other molecules to flow into the cytosolic compartment. This possibility also is unlikely, because any change in lysosomal permeability that released aspartic and serine proteases would likely lead to apoptosis and worsening of the disease seen in various organs (28). In the present studies, however, treatment with CYCLO actually decreased cell death and improved measures of tissue integrity (Figs. 4 and 5).

A third possibility is that CYCLO reaching the late E/L compartment through bulk-phase endocytosis either activated some, as

yet, undescribed secondary C transporter or, more likely, acted in a catalytic fashion to promote C transfer, bypassing the defective function of the mutant NPC1 protein. Originally, it seemed reasonable that during lysosomal processing of CE, the sequence of events was for LAL to release C to the soluble NPC2, which, in turn, would then transfer it to NPC1 for translocation across the limiting membrane. Recent studies, however, have raised the possibility that the direction of C movement may be from LAL to NPC1, from NPC1 to NPC2, and from NPC2 to some as yet undescribed transporter located in the limiting membrane (29, 30). If this scenario is correct, CYCLO might act in the late E/L compartment by shuttling C between LAL and NPC2, thereby bypassing the defective NPC1. This would fully account for the observation that the flow of C out of the late E/L compartment into the metabolically active pool suddenly increased to 233 $mg \cdot d^{-1} \cdot kg^{-1}$, leading to massive expansion of the CE pool, suppression of the SREBP2 system, and activation of certain LXR target genes.

These studies establish that the single dose of CYCLO administered at 7 days of age transiently overcame the transport defect in the late E/L compartment, temporarily suppressing further synthesis of sterol and allowing a major portion of the sequestered pool to be metabolized and excreted from the body. This reduced the total body burden of C by nearly 500 mg/kg after 24 h and by 900 mg/kg after 6 weeks. Even this transient effect markedly reduced the activation and influx of macrophages into the liver and brain, significantly improved liver function and Purkinje cell survival, and, ultimately, led to increased lifespan. The fact that significant alterations in brain biochemistry and nerve cell survival occurred after these injections clearly implied that the reflection coefficient for CYCLO in the central nervous system, although presumably high, was not 1.0. Given these very favorable biochemical and clinical alterations following the single injection, the question arises as to whether repeated injections of CYCLO over time might completely prevent the increase in total body C burden and, essentially, prevent the organ dysfunction seen in NPC disease.

Further, it must be established whether the reflection coefficient for CYCLO in the brain does become 1.0 as the animal ages and, therefore, whether such continuous CYCLO administration must be carried out both systemically, to prevent the lung and liver disease, and into the central nervous system, to halt the neurodegeneration.

Materials and Methods

Animals. WT ($npc1^{+/+}$) and homozygous mutant ($npc1^{-/-}$) mice were generated from heterozygous ($npc1^{+/-}$) animals with a pure BALB/c background (6, 15). Most pups were genotyped at 19 days of age, except in those experiments using 7-day-old animals, where the pups were genotyped at 5 days of age. All animals were housed in plastic colony cages in rooms with alternating 12-h periods of dark and light and were studied in the fed state. For the experiments using 49-day-old mice, there were comparable numbers of males and females in every group. The gender of the mice studied at 8 days of age was not determined. The dark phase began at 24:00 h and lasted 12 h. All experimental protocols were approved by the Institutional Animal Care and Use Committee of the University of Texas Southwestern Medical School.

Treatments and Diets. All animals except the heterozygous breeding stock were fed ad libitum a cereal-based low-cholesterol (0.02% wt/wt) diet (no. 7001; Harlan Teklad) or a ground form of this same diet containing ezetimibe (Schering-Plough Research Institute) (0.0125% wt/wt, providing ≈20 $mg \cdot d^{-1} \cdot kg^{-1}$ bw) on weaning at 19 days of age. The breeding stock was maintained on another formulation containing 0.03% wt/wt cholesterol (no. 7002; Harlan Teklad). Mice were administered a single s.c. injection during the late dark phase at the scruff of the neck at 7 days of age of a 20% (wt/vol in saline) solution of CYCLO (4,000 mg/kg bw) with either 5.6° of substitution (product 332607; Aldrich) or 4.5° of substitution (product H107; Sigma). In some experiments, Allo (P 8887; Sigma) was added to the CYCLO solutions at a concentration of 1.5 mg/ml (25 mg/kg bw) (15, 16). Matching mice injected with saline only served as controls. All mice were studied either 24 h or 42 days later at the end of the dark cycle, when the animals were either 8 days or 49 days old, respectively.

CYCLO Pharmacokinetics. Whole-body CYCLO clearance was measured in 7- and 49-day-old mice using ^{14}C-CYCLO. Aliquots of the stock solution of ^{14}C-CYCLO (1.0 mCi/ml) were diluted with a 20% (wt/vol) solution of nonradiolabeled CYCLO just before administration to the mice, which were subsequently killed at various time points up to 24 h. The proportion of the administered ^{14}C-CYCLO dose that was retained by the body at each time point was determined by scintillation spectrometry after complete chemical digestion of the entire carcass. These data were used to calculate the proportion of the administered dose of ^{14}C-CYCLO that had been cleared from the animal over each respective time interval.

Additional materials and methods are described in supporting information (SI) *Materials and Methods* and Table S1.

ACKNOWLEDGMENTS. The authors thank Heather Waddell, Sean Campbell, and Carolyn Smith for their excellent technical assistance and Kerry Foreman for expert preparation of the manuscript. This work was supported by US Public Health Service Grants RO1 HL-09610 and T32 DK-07745 (to J.M.D., S.D.T., and B.L.), the Moss Heart Fund (J.M.D.), and the Ara Parseghian Medical Research Foundation (J.J.R.). B.L. also received postdoctoral support from a grant by the Ara Parseghian Medical Research Foundation and the Dana's Angels Research Trust.

1. Carstea ED, *et al.* (1997) Niemann-Pick C1 disease gene: Homology to mediators of cholesterol homeostasis. *Science* 277:228–231.
2. Naureckiene S, *et al.* (2000) Identification of *HE1* as the second gene of Niemann-Pick C disease. *Science* 290:2298–2301.
3. Liu B, Xie C, Richardson JA, Turley SD, Dietschy JM (2007) Receptor-mediated and bulk-phase endocytosis cause macrophage and cholesterol accumulation in Niemann-Pick C disease. *J Lipid Res* 48:1710–1723.
4. Blanchette-Mackie EJ (2000) Intracellular cholesterol trafficking: Role of the NPC1 protein. *Biochim Biophys Acta* 1486:171–183.
5. Xie C, Turley SD, Pentchev PG, Dietschy JM (1999) Cholesterol balance and metabolism in mice with loss of function of Niemann-Pick C protein. *Am J Physiol* 276:E336–E344.
6. Loftus SK, *et al.* (1997) Murine model of Niemann-Pick C disease: Mutation in a cholesterol homeostasis gene. *Science* 277:232–235.
7. Xie C, Turley SD, Dietschy JM (1999) Cholesterol accumulation in tissues of the Niemann-Pick type C mouse is determined by the rate of lipoprotein-cholesterol uptake through the coated-pit pathway in each organ. *Proc Natl Acad Sci USA* 96:11992–11997.
8. Pentchev PG, Vanier MT, Suzuki K, Patterson MC (1995) Niemann-Pick disease type C: A cellular cholesterol lipidosis. *The Metabolic and Molecular Bases of Inherited Disease*, eds Scriver CR, *et al.* (McGraw-Hill, New York), 7th Ed, pp 2625–2639.
9. Beltroy EP, Liu B, Dietschy JM, Turley SD (2007) Lysosomal unesterified cholesterol content correlates with liver cell death in murine Niemann-Pick type C disease. *J Lipid Res* 48:869–881.
10. Repa JJ, *et al.* (2007) Liver X receptor activation enhances cholesterol loss from the brain, decreases neuroinflammation, and increases survival of the NPC1 mouse. *J Neurosci* 27:14470–14480.
11. Brown MS, Goldstein JL (1979) Receptor-mediated endocytosis: Insights from the lipoprotein receptor system. *Proc Natl Acad Sci USA* 76:3330–3337.
12. Innerarity TL, Mahley RW (1978) Enhanced binding by cultured human fibroblasts of apo-E-containing lipoproteins as compared with low density lipoproteins. *Biochemistry* 17:1440–1447.
13. Katz Y, Diamond JM (1974) Nonsolvent water in liposomes. *J Membr Biol* 17:87–100.
14. Neufeld EB, *et al.* (1999) The Niemann-Pick C1 protein resides in a vesicular compartment linked to retrograde transport of multiple lysosomal cargo. *J Biol Chem* 274:9627–9635.
15. Liu B, Li H, Repa JJ, Turley SD, Dietschy JM (2008) Genetic variations and treatments that affect the lifespan of the NPC1 mouse. *J Lipid Res* 49:663–669.
16. Griffin LD, Gong W, Verot L, Mellon SH (2004) Niemann-Pick type C disease involves disrupted neurosteroidogenesis and responds to allopregnanolone. *Nat Med* 10:704–711.
17. Goldstein JL, DeBose-Boyd RA, Brown MS (2006) Protein sensors for membrane sterols. *Cell* 124:35–46.
18. Repa JJ, Mangelsdorf DJ (2000) The role of orphan nuclear receptors in the regulation of cholesterol homeostasis. *Annu Rev Cell Dev Biol* 16:459–481.
19. Singaraja RR, *et al.* (2005) Alternate transcripts expressed in response to diet reflect tissue-specific regulation of ABCA1. *J Lipid Res* 46:2061–2071.
20. Beltroy EP, Richardson JA, Horton JD, Turley SD, Dietschy JM (2005) Cholesterol accumulation and liver cell death in mice with Niemann-Pick type C disease. *Hepatology* 42:886–893.
21. Sarna JR, *et al.* (2003) Patterned Purkinje cell degeneration in mouse models of Niemann-Pick type C disease. *J Comp Neurol* 456:279–291.
22. Du H, Duanmu M, Witte D, Grabowski GA (1998) Targeted disruption of the mouse lysosomal acid lipase gene: Long-term survival with massive cholesteryl ester and triglyceride storage. *Hum Mol Genet* 7:1347–1354.
23. Du H, *et al.* (2008) Wolman disease/cholesteryl ester storage disease: Efficacy of plant-produced human lysosomal acid lipase in mice. *J Lipid Res* 49:1646–1657.
24. Szejtli J (1998) Introduction and general overview of cyclodextrin chemistry. *Chem Rev (Washington, DC)* 98:1743–1753.
25. Yancey PG, *et al.* (1996) Cellular cholesterol efflux mediated by cyclodextrins. *J Biol Chem* 271:16026–16034.
26. Christian AE, Haynes MP, Phillips MC, Rothblat GH (1997) Use of cyclodextrins for manipulating cellular cholesterol content. *J Lipid Res* 38:2264–2272.
27. Atger VM, *et al.* (1997) Cyclodextrins as catalysts for the removal of cholesterol from macrophage foam cells. *J Clin Invest* 99:773–780.
28. Stoka V, Turk V, Turk B (2007) Lysosomal cysteine cathepsins: Signaling pathways in apoptosis. *Biol Chem* 388:555–560.
29. Infante RE, *et al.* (2008) NPC2 facilitates bidirectional transfer of cholesterol between NPC1 and lipid bilayers, a step in cholesterol egress from lysosomes. *Proc Natl Acad Sci USA* 105:15287–15292.
30. Xu Z, Farver W, Kodukula S, Storch J (2008) Regulation of sterol transport between membranes and NPC2. *Biochemistry* 47:11134–11143.